J|A|C|S COMMUNICATIONS

Published on Web 02/06/2009

A Spray-Processable, Low Bandgap, and Ambipolar Donor−Acceptor Conjugated Polymer

Timothy T. Steckler,[†] Xuan Zhang,[‡] Jungseek Hwang,[§] Ryan Honeyager,[§] Shino Ohira,[‡] Xiao-Hong Zhang,[¶] Adrian Grant,[¶] Stefan Ellinger,[†] Susan A. Odom,[‡] Daniel Sweat,[‡] David B. Tanner,[§] Andrew G. Rinzler,[§] Stephen Barlow,[‡] Jean-Luc Brédas,[‡] Bernard Kippelen,[¶] Seth R. Marder,*[,‡] and John R. Reynolds*[,†]

The George and Josephine Butler Polymer Research Laboratory, Department of Chemistry, Center for Macromolecular Science and Engineering, University of Florida, Box 117200, Gainesville, Florida 32611, School of Chemistry & Biochemistry and Center for Organic Photonics and Electronics, Georgia Institute of Technology, 901 Atlantic Drive, Atlanta, Georgia 30332, Department of Physics, University of Florida, Box 118440, Gainesville, Florida 32611, School of Electrical and Computer Engineering and Center for Organic Photonics and Electronics, Georgia Institute of Technology, 777 Atlantic Drive NW, Atlanta, Georgia 30332

Received December 7, 2008; E-mail: seth.marder@chemistry.gatech.edu; reynolds@chem.ufl.edu

Narrow bandgap conjugated polymers can provide a unique set of redox and optoelectronic properties, including broad and long wavelength light absorption, solid-state transport of both holes and electrons, and access to multiple charge states in a small potential window. In ground-breaking work, Wudl et al. demonstrated that polyisothianaphthene exhibited a bandgap of ~1 eV due to the appended benzene ring forcing the thiophene into a quinoid-like ground-state geometry.[1] Multiple researchers have also sought to reduce the band gap by using a donor−acceptor (DA) approach.[2] This method has proven to be an effective strategy for tailoring the properties of oligomers and polymers for applications in photovoltaics,[3] OLEDs,[4] electrochromics,[5] and OFETs.[3a,4e,6]

To enhance the D−A interaction and simultaneously produce soluble low band gap polymers, we have utilized the strong donor dithieno[3,2-*b*:2′,3′-*d*]pyrrole (DTP)[6d,7] functionalized with a trialkoxyphenyl group, combined with a strong acceptor based on benzo[1,2-*c*;4,5-*c*′]bis[1,2,5]thiadiazole (BBT)[8] which has been previously used in soluble low band gap polymers for photovoltaic applications.[9] In investigating donor−acceptor−donor (DAD) systems, we have previously used the electron-rich dioxythiophene-based donors with this acceptor; however, the molecules suffer from large dihedral angles which decrease the π conjugation relative to molecules where unsubstituted thiophene flanks the acceptor. For example, using 3,4-ethylenedioxythiophene (EDOT), the λ_{max} for BEDOT-BBT (4,8-bis(2,3-dihydrothieno[3,4-*b*][1,4]dioxin-5-yl)-benzo[1,2-*c*;4,5-*c*′]bis[1,2,5]thiadiazole) (643 nm) is blue-shifted about 0.16 eV compared to BTh-BBT (4,8-dithien-2-yl-2$\lambda^4\delta^2$-benzo[1,2-*c*;4,5-*c*′]bis[1,2,5]thiadiazole) (702 nm).[8b,10] Turning to the fused-ring DTP, this donor provides a high-lying highest occupied molecular orbital (HOMO), planarity for π stacking, and solubility in the polymers due to the long-chain alkoxy substituents.

As illustrated in Figure 1a, we report on the coupling polymerization of the strong donor, *N*-(3,4,5-tris(dodecyloxy)phenyl)-dithieno[3,2-*b*:2′,3′-*d*]pyrrole with a strong acceptor, BThBBT, via Stille methodology,[11] to obtain the lowest bandgap polymer P(DTP-BThBBT) prepared to date that is soluble and spray processable. The polymerization was carried out in THF at reflux for ~2 days, followed by volume reduction and precipitation into methanol. The crude polymer was then purified by Soxhlet extraction with MeOH, hexane, acetone, and $CHCl_3$. The $CHCl_3$ fraction was then reduced in volume, precipitated into methanol, and collected by filtration yielding a black solid with a M_n of 14 K and a PDI of 3.6 (all synthetic and characterization details presented in the Supporting Information).

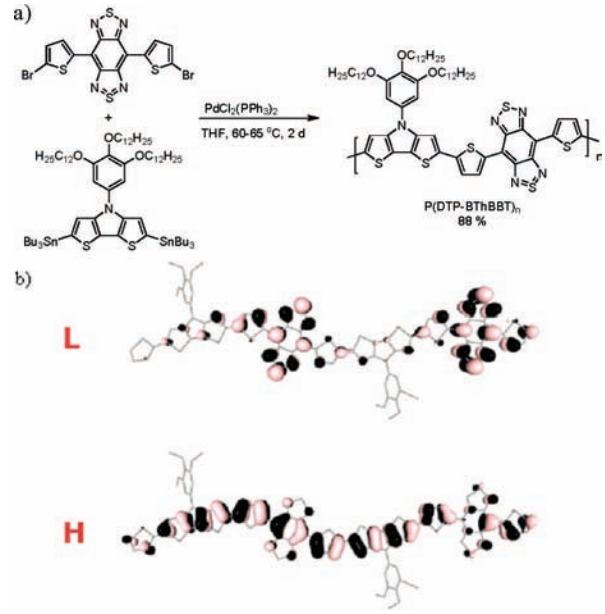

Figure 1. (a) Synthesis of P(DTP-BThBBT); (b) HOMO/LUMO levels of an oligomer (DTP-BThBBT)$_n$ (n = 2) used to calculate the theoretical bandgap.

The geometric structure of P(DTP-BThBBT) and its electronic properties, including the lowest excited-state energies, were calculated at the density functional theory (DFT) and time-dependent (TD)-DFT B3LYP/3-21G* levels using model oligomers (DTP-BThBBT)$_n$ with n = 1, 2, 3, 4, and 6. The HOMO and lowest unoccupied molecular orbitals (LUMO) of (DTP-BThBBT)$_2$ are illustrated in Figure 1b. As in several similar polymers with alternating donor and acceptor units,[12] while the HOMO wave function is delocalized over the whole π system, the LUMO wave function is localized on the acceptor units. The calculated lowest excited-state energy, obtained by extrapolation to $n = \infty$, is 0.50 eV (Supporting Information, Figure S1). Since the lowest lying transition is primarily of HOMO → LUMO character, this points

[†] Department of Chemistry, University of Florida.
[‡] School of Chemistry & Biochemistry and Center for Organic Photonics and Electronics, Georgia Institute of Technology.
[§] Department of Physics, University of Florida.
[¶] School of Electrical and Computer Engineering and Center for Organic Photonics and Electronics, Georgia Institute of Technology.

10.1021/ja809372u CCC: $40.75

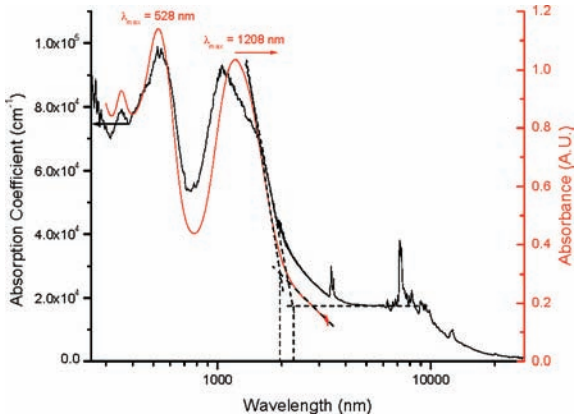

Figure 2. Reflectance spectrum of P(DTP-BThBBT) film on gold (black curve) and absorption spectrum on SWCNT (red curve).

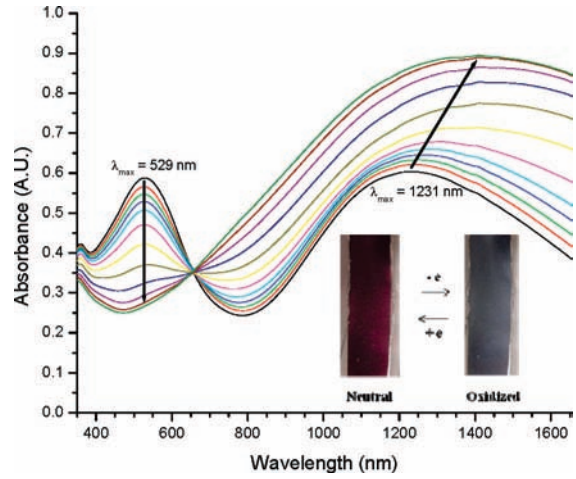

Figure 3. Oxidative spectroelectrochemistry of P(DTP-BThBBT) spray cast on to an ITO coated glass working electrode using a Ag wire pseudoreference electrode calibrated to Fc/Fc^+ and a Pt wire counterelectrode in 0.1 M TBAP/PC. The potential was switched from −0.13 to +0.97 V vs SCE in 100 mV increments. Inset shows a picture of the neutral and oxidized polymer film.

to intramolecular charge-transfer and suggests that P(DTP-BThBBT) will have an especially low onset for optical absorbance.

The theoretical results are confirmed for polymer films spray cast from $CHCl_3$ solutions onto indium tin oxide (ITO), single-walled carbon nanotubes (SWCNT),[13] and gold electrodes on glass for spectral and redox characterization as shown in Figure 2. P(DTP-BThBBT) sprayed onto a SWCNT electrode shows a λ_{max} of 1208 nm with an absorption onset at ∼1967 nm corresponding to a bandgap of ∼0.63 eV determined via the tangent lines (red spectrum). Meanwhile the reflectance spectrum obtained on gold and converted into absorption coefficient for direct comparison (black), allows us to go deeper into the mid-IR for better baseline characterization. The polymer shows an onset of absorption at ∼2260 nm giving a bandgap of 0.54 eV, which is close to the calculated S_1 excited-state energy of 0.50 eV. The reflectance spectrum shows the C−H stretching vibrations (aromatic C−H ∼3100 to 3000 cm^{-1} and alkyl C−H ∼3000 to 2840 cm^{-1}) at ∼3350 to 3550 nm along with the C−H bending modes (∼1450 and 1375 cm^{-1}) between 7100 and 7400 nm. Thermal stability was analyzed by TGA; the polymer showed a 5 wt % loss at 331 and 316 °C under N_2 and air atmospheres, respectively. As another demonstration of stability (Supporting Information Figure S6), P(DTP-BThBBT) was exposed to outdoor (Supporting Information Table S1) light/air conditions and showed only minor changes in the UV−vis absorption spectrum over a period of 7 weeks.

Electrochemistry was carried out on drop-cast films (from $CHCl_3$) on a platinum button working electrode, using a Pt flag counter electrode, and a Ag/Ag^+ (0.01 M $AgNO_3$, 0.1 M TBAP, CH_3CN) reference electrode. Films were repeatedly redox switched in a 0.1 M TBAP/PC (tetrabutylammonium perchlorate/propylene carbonate) solution until reproducible electrochemistry was achieved. Cyclic voltammetry shows an $E_{1/2\ ox}$ of 0.7 V vs SCE and two reductions at $E_{1/2\ red} = -0.50$ and −1.05 V vs SCE (Supporting Information Figure S2). On the basis of the onsets for oxidation (ca. +0.3 V vs SCE, depending upon the method) and reduction (ca. −0.3 V vs SCE) we estimate an electrochemical bandgap of 0.6−0.95 V consistent with the spectral and computational results. Extending the energy levels to vacuum yields an estimated solid-state ionization potential of ca. 5.0−5.1 eV and electron affinity of ca. 4.4−4.2 eV. These values suggest the possibility of facile injection of both holes and electrons from commonly used electrode materials, and, therefore, of ambipolar charge transport.

Oxidative (Figure 3) and reductive spectroelectrochemistry was performed on a film of P(DTP-BThBBT) on ITO after ca. 20 redox cycles. ITO was used as the electrodes in these experiments (the strong absorption of the solvent/electrolyte system beyond 2000 nm makes the use of the SWCNTs less valuable for this experiment). In neutral P(DTP-BThBBT), two absorption bands[5d,14] are observed with peaks at 1231 and 529 nm, corresponding to a purple neutral polymer (see photograph in Figure 3). Upon incremental oxidation, a bleaching of the peak at 529 nm occurs and a broad absorption develops that extends into the IR with a maximum near ∼1400 nm that swamps the neutral polymer's low-energy transition suggesting a p-doped state.[15] This results in a more visibly transparent gray/blue polymer film.

Reductive spectroelectrochemistry (Supporting Information, Figure S3), with incremental potential stepping from the neutral state (+0.05 V vs SCE) to the first reduced state (−0.95 V vs SCE), induces a decrease in intensity of the long wavelength band of the neutral polymer along with the formation of a less intense band at ∼1500 nm attributed to n-type doping.[15] Concurrently, there is an increase in the intensity of the high-energy band at 524 nm (with a 10−15 nm red shift) along with the development of a slight shoulder at 700 nm. This results in a darker purple film in the first reduced state (Supporting InformationFigure S4). When the potential is stepped to the second reduction, the band at ∼1500 nm is fully bleached, while the shoulder from the first reduction develops into a new well-defined peak at 770 nm. This results in a polymer with peaks at ∼535 and ∼770 nm yielding a bright blue/purple film with saturated color (Supporting Information, Figure S4).

Since the electrochemistry and spectroelectrochemistry of P(DTP-BThBBT) showed both p- and n-type doping at moderate potentials, it was though that this polymer might serve as a candidate ambipolar charge-transport material. To investigate the transport properties of P(DTP-BThBBT), top-contact OFETs were prepared on heavily *n*-doped silicon (n^+-Si) substrates with 200-nm-thick thermally grown SiO_2 as gate dielectric ($\varepsilon_r = 3.9$). A 50 nm portion of Au and 5 nm of Ti were deposited (using an e-beam system) on the back of the n^+-Si substrate as a layer to create a better contact of the gate electrode (n^+ doped Si) of the OFET. Ti was used as an adhesion layer for the gold onto to the Si-substrate. The SiO_2 layer was then treated with either a self-assembled monolayer (SAM) of octadecyltrichlorosilane (Q1 devices) or a thin buffer layer of benzocyclobutene (Q2 devices). The P(DTP-BThBBT) layer was then spin-coated on the treated SiO_2 (Q1:OTS, Q2:BCB) at 500 rpm for 60 s in a N_2-filled glovebox from a solution of 10 mg/mL in chlorobenzene. The devices were then completed with 100 nm-

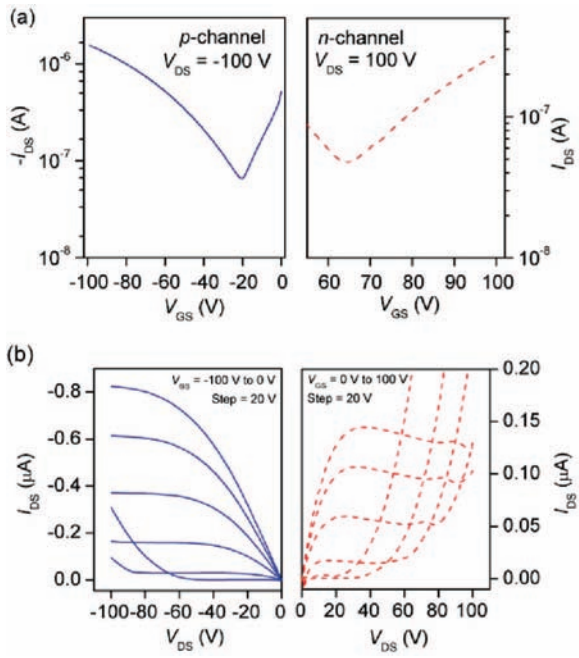

Figure 4. (a) Transfer characteristics of samples Q1 and (b) corresponding output characteristics; p-channel operation (full line in panels a and b) is measured in a device annealed at 110 °C; n-channel operation (dash line in panels a and b) is measured in a device annealed at 150 °C.

thick Al source and drain electrodes through a shadow mask. The channel length and width were $L = 50$ μm and $W = 1000$ μm, respectively.

Clear n-and p-channel behavior was observed on the transfer and output characteristics of devices Q1 and Q2. The electrical characteristics were measured in three sets of samples with identical geometry Q1 and Q2. One set was tested immediately after fabrication. Two other sets were tested after annealing for 30 min at a temperature of 110 or 150 °C. Figure 4 shows the best transfer (Figure 4a) and output characteristics (Figure 4b) measured in samples with geometry Q1. p- and n-Channel electrical characteristics are shown for a sample Q1 annealed at 110 and 150 °C, respectively. Field-effect mobility values of 1.2×10^{-3} and 5.8×10^{-4} cm^2/(V•s) were measured for p-channel and n-channel operation, respectively. In samples Q2, a p-channel field-effect mobility value of 3.7×10^{-5} cm^2/(V•s) was obtained in samples annealed at 110 °C, and the best p-channel field-effect mobility value of 9.2×10^{-5} cm^2/(V•s) was obtained in unannealed samples demonstrating the importance of surface treatment on device performance. Higher charge mobility could be achieved by maximizing the polymer interchain interactions.

In conclusion, a new soluble, spray-processable, donor−acceptor polymer has been synthesized and shows an optical bandgap of 0.5−0.6 eV, which is the lowest value reported for a soluble spray-processable polymer. Four differently colored redox states of the polymer can be accessed at moderate potentials and have good stability. The polymer also shows potential for use in ambipolar OFETs with respectable mobilities for a solution-processed device. We are currently investigating other applications such as detectors and infrared two-photon absorptivity.

Acknowledgment. This work was funded in part by DARPA (N00014-06-1-0897), the Office of Naval Research (at GIT and N00014-08-1-0928), the AFOSR (FA9550-06-1-0192), and the STC Program of the National Science Foundation under Agreement No. DMR-0120967. The solid state device work was performed in part at the Microelectronics Research Center at Georgia Institute of Technology, a member of the National Nanotechnology Infrastructure Network, which is supported by NSF (Grant No. ECS- 03-35765).

Supporting Information Available: Details of experimental results (electrochemical data, theoretical calculations) and synthetic preparation. This material is available free of charge via the Internet at http://pubs.acs.org.

References

(1) (a) Wudl, F.; Kobayashi, M.; Heeger, A. J. *J. Org. Chem.* **1984**, *49*, 3382–3384. (b) Brédas, J. L.; Heeger, A. J.; Wudl, F. *J. Chem. Phys.* **1986**, *85*, 4673–4678. (c) Hoogmartens, I.; Adriaensens, P.; Vanderzande, D.; Gelan, J.; Quattrocchi, C.; Lazzaroni, R.; Brédas, J. L. *Macromolecules* **1992**, *25*, 7347–7356. (d) Kertesz, M.; Choi, C. H.; Yang, S. *Chem. Rev.* **2005**, *105*, 3448–3481.

(2) (a) Brédas, J. L. *J. Chem. Phys.* **1985**, *82*, 3808–3811. (b) Havinga, E. E.; Hoeve, W.; Wynberg, H. *Polym. Bull.* **1992**, *29*, 119–126. (c) Roncali, J. *Chem. Rev.* **1997**, *97*, 173–206. (d) van Mullekom, H. A. M.; Vekemans, J. A. J. M.; Havinga, E. E.; Meijer, E. W. *Mater. Sci. Eng.: R* **2001**, *32*, 1–40. (e) Ajayaghosh, A. *Chem. Soc. Rev.* **2003**, *32*, 181–191.

(3) (a) Zhu, Z.; Waller, D.; Gaudiana, R.; Morana, M.; Muhlbacher, D.; Scharber, M.; Brabec, C. *Macromolecules* **2007**, *40*, 1981–1986. (b) Mammo, W.; Admassie, S.; Gadisa, A.; Zhang, F.; Inganäs, O.; Andersson, M. R. *Sol. Energy Mater. Sol. Cells* **2007**, *91*, 1010–1018. (c) Colladet, K.; Fourier, S.; Cleij, T. J.; Lutsen, L.; Gelan, J.; Vanderzande, D.; HuongNguyen, L.; Neugebauer, H.; Sariciftci, S.; Aguirre, A.; Janssen, G.; Goovaerts, E. *Macromolecules* **2007**, *40*, 65–72. (d) Blouin, N.; Leclerc, M. *Acc. Chem. Res.* **2008**, *41*, 1110–1119. (e) Li, Y.; Zou, Y. *Adv. Mater.* **2008**, *20*, 2952–2958. (f) Wienk, M. M.; Turbiez, M.; Gilot, J.; Janssen, R. A. J. *Adv. Mater.* **2008**, *20*, 2556–2560. (g) Huo, L.; Tan, Z. a.; Wang, X.; Zhou, Y.; Han, M.; Li, Y. *J. Polym. Sci., Part A* **2008**, *46*, 4038–4049.

(4) (a) Chen, M. X.; Perzon, E.; Robisson, N.; Jönsson, S. K. M.; Andersson, M. R.; Fahlman, M.; Berggren, M. *Synth. Met.* **2004**, *146*, 233–236. (b) Kulkarni, A. P.; Kong, X.; Jenekhe, S. A. *Macromolecules* **2006**, *39*, 8699–8711. (c) Kulkarni, A. P.; Zhu, Y.; Babel, A.; Wu, P.-T.; Jenekhe, S. A. *Chem. Mater.* **2008**, *20*, 4212–4223. (d) Yang, Y.; Farley, R. T.; Steckler, T. T.; Eom, S.-H.; Reynolds, J. R.; Schanze, K. S.; Xue, J. *Appl. Phys. Lett.* **2008**, *93*, 163305. (e) Zaumseil, J.; McNeill, C. R.; Bird, M.; Smith, D. L.; Ruden, P. P.; Roberts, M.; McKiernan, M. J.; Friend, R. H.; Sirringhaus, H. *J. Appl. Phys.* **2008**, *103*, 064517.

(5) (a) Thompson, B. C.; Kim, Y. G.; McCarley, T. D.; Reynolds, J. R. *J. Am. Chem. Soc.* **2006**, *128*, 12714–12725. (b) Gunbas, G. E.; Durmus, A.; Toppare, L. *Adv. Mater.* **2008**, *20*, 691–695. (c) Beaujuge, P. M.; Ellinger, S.; Reynolds, J. R. *Nat. Mater.* **2008**, *7*, 795–799. (d) Beaujuge, P. M.; Ellinger, S.; Reynolds, J. R. *Adv. Mater.* **2008**, *20*, 2772–2776.

(6) (a) Mas-Torrent, M.; Rovira, C. *Chem. Soc. Rev.* **2008**, *37*, 827–838. (b) Usta, H.; Facchetti, A.; Marks, T. J. *J. Am. Chem. Soc.* **2008**, *130*, 8580–8581. (c) Letizia, J. A.; Salata, M. R.; Tribout, C. M.; Facchetti, A.; Ratner, M. A.; Marks, T. J. *J. Am. Chem. Soc.* **2008**, *130*, 9679–9694. (d) Liu, J.; Zhang, R.; Sauvé, G.; Kowalewski, T.; McCullough, R. D. *J. Am. Chem. Soc.* **2008**, *130*, 13167–13176. (e) Zhu, Y.; Champion, R. D.; Jenekhe, S. A. *Macromolecules* **2006**, *39*, 8712–8719. (f) Yamamoto, T.; Yasuda, T.; Sakai, Y.; Aramaki, S. *Macromol. Rapid Commun.* **2005**, *26*, 1214–1217.

(7) (a) Ogawa, K.; Rasmussen, S. C. *J. Org. Chem.* **2003**, *68*, 2921–2928. (b) Ogawa, K.; Rasmussen, S. C. *Macromolecules* **2006**, *39*, 1771–1778. (c) Pappenfus, T. M.; Hermanson, B. J.; Helland, T. J.; Lee, G. G. W.; Drew, S. M.; Mann, K. R.; McGee, K. A.; Rasmussen, S. C. *Org. Lett.* **2008**, *10*, 1553–1556.

(8) (a) Karikomi, M.; Kitamura, C.; Tanaka, S.; Yamashita, Y. *J. Am. Chem. Soc.* **1995**, *117*, 6791–6792. (b) Kitamura, C.; Tanaka, S.; Yamashita, Y. *Chem. Mater.* **1996**, *8*, 570–578.

(9) (a) Bundgaard, E.; Krebs, F. C. *Sol. Energy Mater. Sol. Cells* **2007**, *91*, 1019–1025. (b) Bundgaard, E.; Krebs, F. C. *Macromolecules* **2006**, *39*, 2823–2831.

(10) Steckler, T. T.; Abboud, K. A.; Craps, M.; Rinzler, A. G.; Reynolds, J. R. *Chem. Commun.* **2007**, 4904–4906.

(11) Bao, Z.; Chan, W. K.; Yu, L. *J. Am. Chem. Soc.* **1995**, *117*, 12426–12435.

(12) Zhou, E.; Nakamura, M.; Nishizawa, T.; Zhang, Y.; Wei, Q.; Tajima, K.; Yang, C.; Hashimoto, K. *Macromolecules* **2008**, *41*, 8302–8305.

(13) Wu, Z.; Chen, Z.; Du, X.; Logan, J. M.; Sippel, J.; Nikolou, M.; Kamaras, K.; Reynolds, J. R.; Tanner, D. B.; Hebard, A. F.; Rinzler, A. G. *Science* **2004**, *305*, 1273–1276.

(14) Salzner, U.; Köse, M. E. *J. Phys. Chem. B* **2002**, *106*, 9221–9226.

(15) Dubois, C. J.; Abboud, K. A.; Reynolds, J. R. *J. Phys. Chem. B* **2002**, *108*, 8550–8557.

JA809372U